

NOVEL TECHNIQUES CHARACTERIZING SUBSURFACE FATIGUE CRACK GENERATION AND CRACK GROWTH IN MARTENSITE STEELS

H. SUZUKI¹, O. UMEZAWA^{1,4*}, M. HAMADA¹, H. YOKOTA^{2,4}, K. KIDA^{3,4}

¹*Yokohama National University; Yokohama, Japan, *O. Umezawa, e-mail: umezawa@ynu.ac.jp*

²*RIKEN; Wako, Japan*

³*Kyushu University; Fukuoka, Japan*

⁴*“Fundamental Studies on Technologies for Steel Materials with Enhanced Strength and Functions” Consortium of JRCM (The Japan Research and Development Center for Metals)*

ABSTRACT: Novel systems have employed to clarify the substance crack generation and crack growth mechanisms under contact fatigue for martensite steels. Advantages to characterize fatigue crack growth by stress intensity calculation, local strain distribution by electron backscattering diffraction, 3D structure of inclusions by micro slicer system and plastic deformations around crack tip by scanning Hall-probe microscopy have been studied.

KEY WORDS: fatigue, subsurface crack, crack growth, misorientation, precise cutting, plastic zone

マルテンサイト鋼における内部疲労き裂形成とき裂成長挙動の解析

概要: マルテンサイト鋼の接触疲労における内部き裂発生とき裂成長を明らかにするために、種々の解析方法の適用を検討している。すなわち、応力拡大係数モデリングによるき裂成長、EBSD法による局所ひずみ分布解析、3次元内部構造観察装置による介在物の3次元観察、磁場顕微鏡によるき裂前方の塑性域の同定についてである。

NOVÉ TECHNIKY K OBJASNĚNÍ VZNIKU A RŮSTU PODPOVRCHOVÝCH ÚNAVOVÝCH TRHLIN V MARTENZITICKÝCH OCELÍCH

ABSTRAKT: Pro objasnění vzniku pod povrchového únavových trhlin a mechanismu jejich růstu v podmínkách kontaktní únavy byly využity nové techniky. V rámci řešení byly studovány výhody charakterizace růstu únavových trhlin pomocí výpočtů koncentrace napětí a také distribuce lokální deformace pomocí difrakce zpětně odražených elektronů. Zároveň byla hodnocena 3D struktura inkluzí, a to pomocí systému mikro řezů, a rovněž plastická deformace na čele trhliny s využitím metody SHPM (scanning Hall probe microscopy).

1 INTRODUCTION

Subsurface fatigue crack generation (fish-eye fracture) which occurs with the existence of inclusions is dominant in long-life range for martensite steels.[1] As the first approximation, it needs to calculate stress intensity of growing crack rounded a complex stress field. Through a series of finite element analyses, the influence function method is suitable to solve stress intensity around the crack front in detail [2]. Shiratori *et al.* [2,3] have developed a software system “SCAN” based on the linear fracture mechanics and have installed a simple transition model based on the standards of ASME Code Section XI [4] and WES 2805 Standard [5] in the system for subsurface crack. Elastic incompatibility due to heterogeneous microplasticity, however, plays an important role on the crack generation and growth. Thus the integrated study between mechanics and metallurgy is needed to clarify their mechanism. In the present study, novel analyses have employed to take local stress distribution into consideration for contact fatigue of martensite steels.

2 OUTLINE OF TECHNIQUES

2.1 Calculation of stress intensity factor and modeling of crack growth

Fatigue crack initiation sites and fracture surfaces were analyzed by scanning electron microscopy (SEM). The crack length, $2a$, crack width, $2c$, and distance from specimen surface to center of ellipse, d , were determined, where the direction of crack length was parallel to the initial crack propagating direction. Maximum fatigue crack size in Stage II was taken from the ripple mark on fracture surface. Thus both initial and maximum crack sizes were experimentally given. A linear fracture mechanics program, SCAN subsurface crack version [3], was adopted to evaluate the ΔK of a subsurface crack.

Adopting the calculated stress intensity range results in the modeling of fatigue crack growth by integral of the Paris equation [6] as follows:

$$\frac{da}{dN} = C(\Delta K)^m \quad (1)$$

where C and m are constants. The constants in the Eq.(1) were chosen as $C=5.07 \times 10^{-9}$ and $m=3.21$. Those were resulted from crack propagating tests in the reference [7]. Then the crack propagating life, N_p , was estimated by the crack growth modeling. The number of cycles to failure, N_f , was obtained in the experimental. In the present study, the crack initiation life, N_i , is defined as

$$N_i = N_f - N_p \quad (2)$$

2.2 Misorientation analyses by electron backscattering diffraction

A focused Ar ion-beam sectioning machine was employed to prepare samples with less strained flat surface. Electron backscattered diffraction (EBSD) pattern analysis with scanning electron microscopy (SEM) was performed to determine misorientation distribution. A data set of point analyses with every $0.1 \mu\text{m}$ beam

scanning in hexagonal grids yielded maps for image quality (IQ), inverse pole figure (IPF), grain orientation spread (GOS), grain average misorientation (GAM) and kernel average misorientation (KAM). The IQ represents diffraction pattern strength and reflects on strain field. The GOS indicates the average orientation spread of data with n points in a grain as described by Eq.(3).

$$GOS = \frac{\sum_{i,j=1}^n \alpha_{ij(i \neq j)}}{n(n-1)} \quad (3)$$

The GAM is the average misorientation of every point in a grain. Eq.(4) gives for the number of boundaries with m .

$$GAM = \frac{\sum_{i=1}^m \alpha_i^A}{m} \quad (4)$$

The KAM is the average misorientation of each point in a grain.

2.3 Micro slice of inclusion

An ultrasonic elliptical vibration cutting device has been installed into the Riken micro slicer system to make cutting surface of steels mirror. Tab.1 summarizes the specification of the device. The new precise cutting technique gives a three dimensional (3D) observation. Cutting for an inclusion in bearing steel SUJ2 was done with the conditions of 2 μm in vibration amplitude, 2 μm in depth, 1000 mm/min in speed and 5-10 μm per path.

Tab.1: Specification of ultrasonic elliptical vibration cutting device

Ultrasonic generator	Frequency	39±1.5 kHz
	Amplitude control	axis / flexure
	Output	45 W (max)
Vibrator	Model	PZT elliptical vibrator
	Edge height	29±1.0
	Tool	Single crystal diamond

2.4 Scanning Hall-probe microscopy

A scanning Hall-probe microscope with a single axial sensor was employed to analyze plastic deformation around growing crack tip in bearing steel SUJ2 in the air. This is non-distractive method and dynamical monitoring is available. The region of analysis was 10 μm ×10 μm in the present study.

3 RESULTS AND DISCUSSION

3.1 Subsurface crack generation and crack growth

The samples failed by subsurface crack initiation in flexspline (SNCM439 martensite steel) were chosen for the fatigue damage analysis. Crack initiation site (Stage I) shown in Fig.1 was determined as MnS inclusion. Crack growth regime (Stage II) is clearly seen.

Then we estimate the number of cycles in crack propagation stage by SCAN under various stress condition such as simple tension, shear, etc. The cycles depended on stress models rather than stress ratio. It will help to deduce a complex stress field around growing crack.

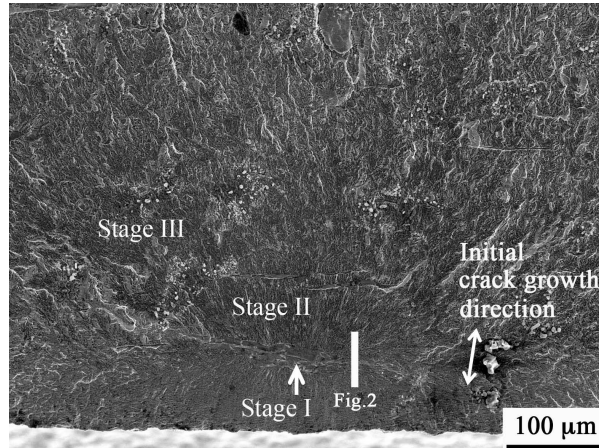


Fig.1: A secondary electron image of fatigue fracture surface (250Nm, $N_f=1.31 \times 10^6$ cycles).

3.2 Local deformation gradient generated by fatigue damage

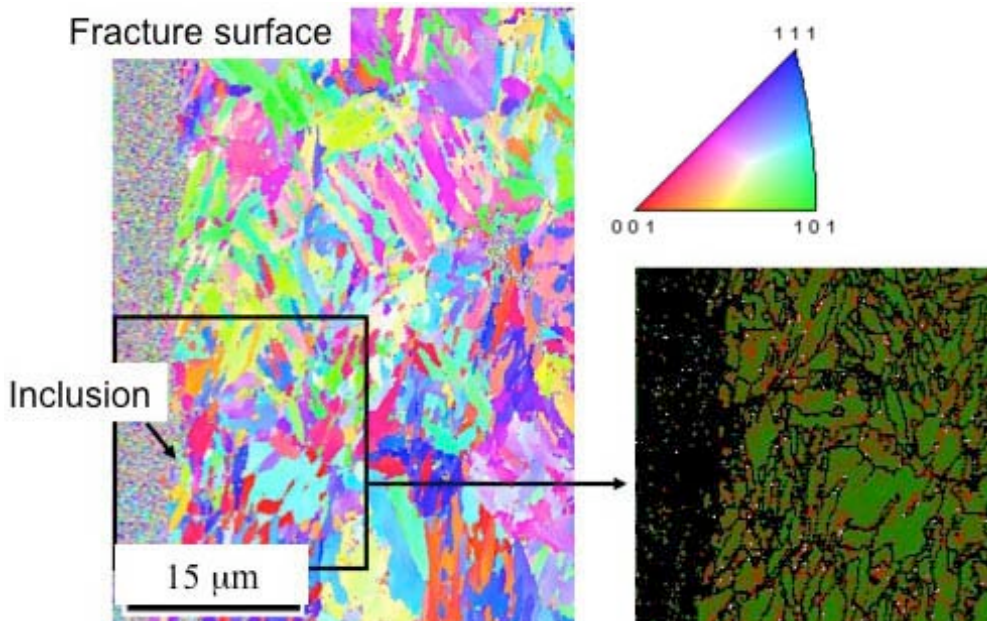


Fig.2: Inverse pole figure map in the cross section shown in Fig.1 and magnified image of KAM.

Fig.2 shows orientation maps at the cross section of fracture surface shown in Fig.1. A local misorientation distribution in the vicinity of grain boundaries was detected in the KAM map as shown in the figure. It means that a crystal rotation typically occurs near grain boundary and results in the formation of localized strain incompatibility near grain boundary. The misorientation of GAM was higher at near the inclusion as from 1 to 1.5 degree.

3.3 Three dimensional morphology of inclusion

Fig.3 shows an example of 3D construction for an inclusion in the bearing steel. Such inclusions with several tens of micro meter in size were detected. The resolution of 3D construction for inclusions was $0.2 \times 0.2 \times 0.5$ [$\mu\text{m}/\text{voxel}$] at the finest observation condition.

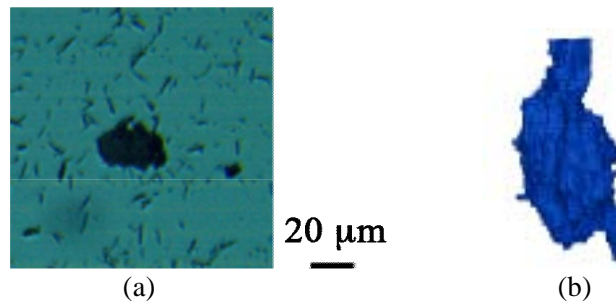


Fig.3: An example of cutting surface image data (a) and 3D construction of an inclusion (b).

3.4 Magnetic field around crack tip

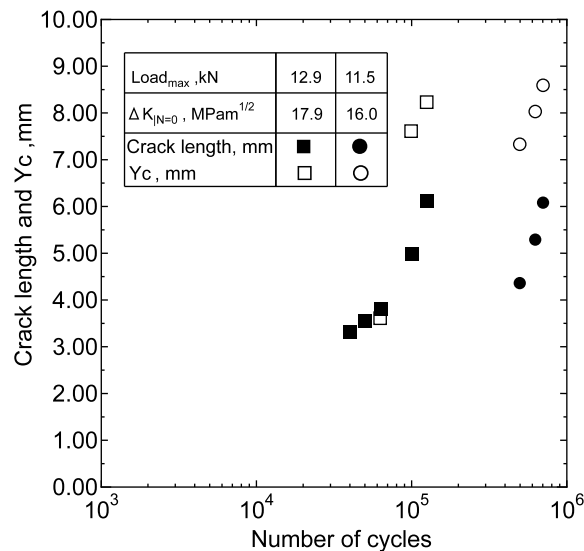


Fig.4: Crack growth (solid plots) and leading edge of plastic zone (open plots) estimated by magnetic flux density with cycles.

Dynamical change of plastic zone in front of growing crack tip was successfully monitored by the scanning Hall-probe microscopy for the bearing steel. Fig.4 shows that the plastic zone length estimated by magnetic flux density, Y_c , is increased as cycles and higher than crack length.

4 SUMMARY

Novel systems have successfully employed to characterize subsurface crack growth, local strain distribution, 3D structure of inclusions and plastic zone around crack tip. In the case of rolling contact fatigue, high compressive stress is introduced in the material. Furthermore a lot of small crack generated near inclusion is retained during cycles. Therefore the systems will have an advantage to clarify the mechanisms of fatigue crack generation and growth.

Acknowledgement

This study has carried out as a part of research activities of "Fundamental studies on technologies for steel materials with enhanced strength and functions" by consortium of the Japan Research and Development Center of Materials. Financial support from New Energy and Industrial Technology Development Organization is gratefully acknowledged.

5 REFERENCES

- [1] Umezawa, O., Nagai, K.: *ISIJ International*, 7, 1997, 1170
- [2] SHIRATORI, M.: In: *Current Topics in Computational Mechanics*, eds. J.F. Cory, Jr. and J.L. Gordon, ASME, 1995, 357
- [3] NAKANISHI, S., IWAMATSU, F., SHIRATORI, M., MATSUSHITA, H.: In: *Proc. Pressure Vessels and Piping 2006*, ASME, 2006, 1
- [4] *ASME Code Section XI*, Rules for in-service inspection of nuclear power plant components, American Society of Mechanical Engineers
- [5] *WES 2805-1997*, Method of assessment for flaws in fusion welded joints with respect to brittle fracture and fatigue crack growth
- [6] PARIS, P.C., ERDOGAN, F.: *Trans. ASME Ser. D, J..Basic Eng.*, 85, 1963, 528
- [7] FUKUSHIMA, A., MISAWA, T., KODAMA, S.: *J. Jpn. Soc. Mech. Eng. A*, 51, 1985, 2684-2691